Biomedicine & Pharmacotherapy 151 (2022) 113171

Contents lists available at ScienceDirect

Biomedicine & Pharmacotherapy

journal homepage: www.elsevier.com/locate/biopha

Galectin-9 supports primary T cell transendothelial migration in a glycan and integrin dependent manner

Adel Abo Mansour [a,b,1], Federica Raucci [c,1], Mustafa Sevim [a,d], Anella Saviano [c], Jenefa Begum [a], Zhaogong Zhi [a], Laleh Pezhman [a], Samantha Tull [a], Francesco Maione [c,*], Asif Jilani Iqbal [a,c,**]

[a] Institute of Cardiovascular Sciences (ICVS), College of Medical and Dental Sciences, University of Birmingham, Birmingham, United Kingdom
[b] Department of Clinical Laboratory Sciences, College of Applied Medical Sciences, King Khalid University, Abha, Saudi Arabia
[c] ImmunoPharmaLab, Department of Pharmacy, School of Medicine and Surgery, University of Naples Federico II, Naples, Italy
[d] Physiology Department, School of Medicine, Marmara University, İstanbul, Turkey

ARTICLE INFO

Keywords:
T cells
Galectin-9 (Gal-9)
Leukocyte trafficking
Recruitment
Inflammation
Chemotaxis

ABSTRACT

Adaptive immunity relies on the efficient recruitment of T cells from the blood into peripheral tissues. However, the current understanding of factor(s) coordinating these events is incomplete. Previous studies on galectin-9 (Gal-9), have proposed a functionally significant role for this lectin in mediating leukocyte adhesion and transmigration. However, very little is known about its function in T cell migration. Here, we have investigated the role of the Gal-9 on the migration behaviour of both human primary $CD4^+$ and $CD8^+$ T cells. Our data indicate that Gal-9 supports both $CD4^+$ and $CD8^+$ T cell adhesion and transmigration in a glycan dependent manner, inducing L-selectin shedding and upregulation of LFA-1 and CXCR4 expression. Additionally, when immobilized, Gal-9 promoted capture and firm adhesion of T cells under flow, in a glycan and integrin-dependent manner. Using an *in vivo* model, dorsal air pouch, we found that Gal-9 deficient mice display impaired leukocyte trafficking, with a reduction in pro-inflammatory cytokines/chemokines generated locally. Furthermore, we also demonstrate that Gal-9 inhibits the chemotactic function of CXCL12 through direct binding. In conclusion, our study characterises, for the first time, the capture, adhesion, and migration behaviour of $CD4^+$ and $CD8^+$ T cells to immobilised /endothelial presented Gal-9, under static and physiological flow conditions. We also demonstrate the differential binding characteristics of Gal-9 to T cell subtypes, which could be of potential therapeutic significance, particularly in the treatment of inflammatory-based diseases, given Gal-9 ability to promote apoptosis in pathogenic T cell subsets.

1. Introduction

Physiological and pathological processes, including the development of immune cells, host defence, and inflammation are highly associated with leukocyte recruitment. For example, T and B cell adaptive immune responses require lymphocyte trafficking between the bone marrow, primary and secondary lymphoid organs and peripheral tissues using blood as a vehicle for extravasating through the endothelium [1–3].

Abbreviations: CXCL-12, C-X-C Motif Chemokine Ligand 12; CXCR4, C-X-C Motif Chemokine Receptor 4; EC, endothelial cells; EC_{50}, half maximal effective concentration; FSC, Forward scatter; Gals, Galectins; Gal-9KO, Galectin-9 knockout; HDBECs, human dermal blood endothelial cells; HUVECs, human umbilical vein endothelial cells; ICAM, intercellular adhesion molecule; IFN-γ, Interferon-gamma; IL, Interleukin; LFA-1, Lymphocyte function-associated antigen 1; MIP-1α, Macrophage Inflammatory Protein-1 Alpha; MMRRC, Mutant Mouse Resource and Research Center; PBMC, Human peripheral blood mononuclear cell; PD-1, programmed cell death protein 1; PFA, Paraformaldehyde; RANTES, regulated upon activation, normal T Cell expressed and presumably secreted; rh, recombinant human; SARS-CoV-2, severe acute respiratory syndrome coronavirus 2; SSC, side scatter; Th, T helper; Tim-3, T cell immunoglobulin mucin-3; TNF-α, tumor necrosis factor alpha; T-reg, regulatory T cells; VCAM, vascular cell adhesion molecule; WT, wild type.

* Correspondence to: ImmunoPharmaLab, Department of Pharmacy, School of Medicine and Surgery, University of Naples Federico II, Via Domenico Montesano 49, 80131 Naples, Italy.

** Corresponding author at: Institute of Cardiovascular Sciences (ICVS), College of Medical and Dental Sciences, University of Birmingham, Birmingham, United Kingdom.

E-mail addresses: francesco.maione@unina.it (F. Maione), A.J.Iqbal@bham.ac.uk (A.J. Iqbal).

[1] These authors share first authorship

https://doi.org/10.1016/j.biopha.2022.113171
Received 12 May 2022; Accepted 22 May 2022
Available online 25 May 2022

However, aberrant lymphocyte trafficking is associated with the onset of chronic inflammation which is a hallmark of a range of conditions including atherosclerosis, rheumatoid arthritis, and chronic transplant rejection [4–6].

Leukocyte trafficking is influenced by numerous factors such as hemodynamic forces, endogenous pro- and anti-inflammatory molecules, in a multistep cascade within the vasculature including capture/rolling, firm adhesion, intraluminal crawling and transmigration [7]. Several key adhesion molecules have been identified at various stages of the cascade, *e.g.*, selectins and integrins, which have been shown to play critical roles [8]. Galectins (Gals), a family of β-galactoside binding proteins with a broad range of physiological functions including cell proliferation, apoptosis, platelet activation, signal transduction, and structural functions, have also been proposed to be functionally significant in mediating leukocyte adhesion and transmigration [9,10]. In the context of inflammation and leukocyte migration, Gal-1, − 3, − 8 and − 9 are amongst the most intensively investigated members with reported pro- or anti-adhesive properties [11–14].

In the present study, we focused on Gal-9, a tandem-repeat type member with two distinct carbohydrate recognition domains joined by a short linker region [1]. Formerly, Gal-9 has been illustrated as an immunoregulatory protein with roles attributed to leukocyte activation and apoptosis. Elevated circulating levels of Gal-9 have been reported in various inflammatory diseases such as large artery atherosclerotic stroke [15], and severe acute respiratory syndrome coronavirus 2 (SARS-CoV-2) infection [16]. In the context of leukocyte trafficking, Gal-9 was originally identified as an eosinophil chemoattractant termed 'Ecalectin' produced by activated T cells and was shown to promote eosinophil adhesion to endothelial cells *in vitro* [17]. Recently, Gal-9 has been reported to mediate monocyte chemotaxis *in vitro* without inflammatory stimuli and monocyte/macrophage infiltration into mouse joints following intra-articular injection with recombinant Gal-9 [18]. In B cells, Gal-9 was shown to promote adhesion to vascular endothelial cells (EC) under flow, but attenuate transendothelial migration of B cells [19]. More recently, our group demonstrated Gal-9 as a direct capture and activation molecule for human neutrophils inducing migration both *in vitro* and *in vivo* [20].

In context of T cell biology, it has been shown that Gal-9 is capable of modulating T cell selection during development and maturation [21,22], as well as the differentiation and expansion of naïve-$CD4^+$ T cells towards a regulatory T cell (T-reg) phenotype [23]. Moreover, it is well documented that Gal-9 interacts with inhibitory T cell receptors, programmed cell death protein 1 (PD-1) and T cell immunoglobulin mucin-3 (Tim-3), to regulate T helper (Th) 1 and Th17 cell death [24]. Over the last two decades, there has been a steady rise in the number of publications detailing the involvement of galectins in widespread physiological functions, including inflammation and immune responses, however, to the best of our knowledge, very little is known about the role of Gal-9 expression in the vascular wall in the context of primary human T cell recruitment. One study which utilised T cell lines (*e.g.* Jurkat) suggests an increase in adhesion to immobilised Gal-9 and ECs under static conditions *in vitro* [17], however, far more convincing evidence with greater pathophysiological relevance is required. Therefore, this study aimed to characterise the role of Gal-9 in $CD4^+$ and $CD8^+$ T cell recruitment under homeostatic and inflammatory settings.

2. Materials and methods

2.1. Reagents

A stable linker-less isoform of recombinant human Gal-9 (GalPharma, Japan) was used throughout as previously described [25]. Removal of the linker region increases the stability of the protein as the linker peptide is susceptible to proteolysis.

2.2. Human blood collection

Blood was collected from healthy volunteers into 10 ml EDTA coated tubes. Written informed consent was obtained from all donors and approval for this study was granted by the University of Birmingham Local Ethical Review Committee (ERN_18 −0382).

2.3. Human peripheral blood mononuclear cell (PBMC) isolation

Human peripheral blood mononuclear cell (PBMC) were isolated as previously described [26]. Briefly, 5 ml of whole blood was layered over an equal volume of Histopaque-1077 (Sigma-Aldrich, U.K.) and centrifuged at 2500 g for 30 min at RT. PBMC layer was transferred into a 15 ml falcon tube and an equal volume of PBS without Ca^{2+} and Mg^{2+} was added to avoid cell activation. Tubes were gently inverted and centrifuged at 1500 g for 5 min at RT. Supernatants were discarded by aspiration and cell pellets were resuspended in 1 ml PBS without Ca^{2+} and Mg^{2+}.

2.4. Human $CD4^+$ and $CD8^+$ subsets isolation

PBMCs were separated as described above and both $CD4^+$ and $CD8^+$ T cell subsets were isolated by negative selection using a commercial kit (Miltenyi, Biotec, Germany). Briefly, PBMCs were incubated with biotin antibody cocktail for 5 min at 4 °C to bind with all cells apart from T cells, followed by incubation with anti-$CD4^+$ or anti-$CD8^+$ microbeads for 10 min at 4 °C. Cells were then added to a MACS LS separation column. Cells recovered from the flow through were the enriched $CD4^+$ and $CD8^+$ T cell fraction. Cells were stained and analysed by flow cytometry to check the purity of isolation.

2.5. Flow Cytometry

To determine the surface binding of Gal-9 to T cells, PBMCs (1×10^6/ per sample) were incubated with or without Gal-9 at several concentrations in the presence or absence of lactose (25 mM, 5989–81–8 Sigma) for 20 min at RT. PBMCs were washed and incubated with anti-human Gal-9 (9M1–3; 1:50, eFluor 660, eBioscience), CD4 (RPAT4; 1:50, eFluor 700, eBioscience), CD8 (OKT3;1:50, eFluor 405, eBioscience) for 20 min at 4 °C. PBMCs were washed again and then fixed in 1% Paraformaldehyde (PFA) for storage before analysis. To investigate the endogenous intracellular expression of Gal-9 in T cell subsets, surface markers were stained first and cells fixed as described previously before permeabilisation (Invitrogen permeabilisation kit, Invitrogen, USA). During permeabilisation, cells were incubated with Gal-9 antibody for 20 min at 4 °C, followed by washing and fixation in 1% PFA for storage before analysis. To measure the effect of exogenous Gal-9 on L-selectin, Lymphocyte function-associated antigen 1 (LFA-1), and C-X-C Motif Chemokine Receptor 4 (CXCR4) expression, PBMCs were isolated as previously described, and the cells were incubated with several concentrations of Gal-9 for 20 min at RT before washing. PBMCs were then stained with the following antibodies: zombie viability dye (423101; 1:200), CD4, CD8, L selectin (DREG-56; 1:50, BV421, Biolegend), LFA-1 (m24; 1:100, PeCy7, eBioscience), and CXCR4 (1:50 CEW33D, PeCy7, eBioscience) for 20 min at 4 °C and then washed and fixed in 1% PFA. After staining, samples were evaluated using the BD LSRFortessa X-20 flow cytometer (BD Biosciences, USA). The flow cytometry data was analysed using FlowJo 7.6.

2.6. Primary human dermal blood endothelial cells

Commercially sourced primary human dermal blood endothelial cells (HDBECs) were cultured in endothelial cell growth medium MV (PromoCell, Heidelberg, Germany). HDBECs were seeded into 12-well tissue culture plates after 4 passages at a seeding density yielding confluent monolayers. HDBEC monolayers were washed in endothelial

cell growth medium MV warmed to 37 °C and simulated with tumor necrosis factor alpha (TNF-α) (Sigma-Aldrich, Poole, UK; 100 U/ml) and Interferon-gamma (IFN-γ) (Sigma-Aldrich, Poole, UK; 10 ng/ml) (Sigma-Aldrich, Poole, UK) in presence or absence of Gal-9 for 24 h. Cells were then incubated with antibodies for intercellular adhesion molecule (ICAM) (BBIG-V3; 1:50, APC, BD Biosciences), vascular cell adhesion molecule (VCAM) (3E2; 1:50, FITC, BD Biosciences), and Gal-9 (9M1–3; 1:50, eFluor 660, eBioscience) for 20 min at 4 °C. HDBEC were washed again and then fixed in 1% PFA for storage before analysis.

2.7. Static adhesion assay

HDBEC were seeded before being stimulated with TNF-α (100 U/ml) and IFN-γ (10 ng/ml) (Sigma-Aldrich, Poole, UK) for 24 h. $CD4^+$ and $CD8^+$ T cells were isolated from healthy volunteers as described above. Cells were diluted to 1×10^6 cells/ml in M199 media and treated with or without Gal-9 for 20 min at RT prior to being added to activated HDBEC for 20 min at 37 °C. In some assays HDBEC were treated with Gal-9 prior to the addition of T cells. Wells were washed twice with PBS to remove unbound cells and fixed with 2% glutaraldehyde for 10 min at RT. Glutaraldehyde was removed with several 1 ml washes of PBS (with Ca^{2+} and Mg^{2+}). Images were taken at five different fields in the centre of each well, and quantification was performed using Image-pro 6.0 software.

2.8. Gal-9 Knock down

HDBEC (Promocell) were transfected at a density of 50,000 cells per well. SiRNA against Gal-9 (Qiagen; FlexiTube GeneSolution GS3965 for LGALS9) and scrambled control were used at 50 nM in Opti-MEM medium and RNAi lipofectamine (Life Technologies Invitrogen Compounds). This mixture was incubated for 10 min at RT before being added to HDBECs for 4 h at 37 °C. Post-transfection, HDBEC were washed with complete media ECGM-MW and incubated at 37 °C for a further 48 h. Post-48 h confluent HDBEC monolayers were cytokine stimulated using TNF-α (100 U/ml; Sigma-Aldrich) diluted in ECGM-MW for 4 h at 37 °C. The extent of Gal-9 knockdown on HDBEC was evaluated by flow cytometry. Briefly, HDBEC were fixed and permeabilised using a commercial kit (eBioscience) and stained with Gal-9 (9M1–3), eFluor 660 (eBioscience) for 20 min at 4 °C. Cells were then washed, fixed and acquired using flow cytometry.

2.9. Flow Adhesion Assay

Gal-9 was incubated on Ibidi chambers (Ibidi, Germany) at different concentrations for 1 h and then blocked using 1.5% BSA for 1 h at 37 °C. $CD4^+$ and $CD8^+$ were isolated from whole blood as previously described at concentration of 1×10^6 cells/ml. The cells are treated with or without lactose, or soluble Tim-3 (2365-TM-050,RD,USA) for 20 min at RT. $CD4^+$ and $CD8^+$ were perfused for 4 min over the immobilised Gal-9 at a flow rate of 0.4 ml/min at 37 °C which provided a wall shear stress of 0.05 Pa. After 4 min perfusion of cells was stopped and a wash out period of 1 min was performed before 7 distinct regions across the centre of the channel were imaged. Quantification of adherent cells was performed with Image-pro 6.0 software.

2.10. Animals

All animal experiments were designed and performed in accordance with Home Office regulations under the licence P50CB9C61. Galectin-9 knockout (Gal-9KO) mice (B6(FVB)- Lgals9tm1.1Cfg/Mmucd, RRID: MMRRC_031952-UCD) were received the Mutant Mouse Resource and Research Center (MMRRC) at University of California at Davis, an NIH-funded strain repository, donated to the MMRRC by Jim Paulson, Ph.D., The Scripps Research Institute, and kept in an animal care facility under controlled temperature, humidity, on a 12 h light/dark cycle, with *ad libitum* access to water and standard laboratory chow diet. C57BL/6 J were used as wild type (WT) controls and were purchased from Charles River UK. In line with the ARRIVE guidelines and the principles of 3Rs on the use of minimal number of animals required for experimentation we performed a power calculation prior to our experiments. We used previous data generated from our lab to determine our desired effect size and based on the power calculation a sample size of six mice per group was required to achieve a statistical significance of 5%.

2.11. Air pouch model

Dorsal air pouches were prepared by injection of 2.5 ml of air on day 0 and day 3 as previously described [27]. On day 6, mice received 500 μg of Zymosan (Millipore-Sigma, Burlington, MA, USA) in 500 μl PBS. Mice were sacrificed after 24 h and air pouches were lavaged with 2 ml of PBS containing 50 U/ml heparin and 3 mM EDTA. Lavage fluids were centrifuged at 220g for 10 min at 4 °C to separate the exudates from the recruited cells. Inflammatory exudates were collected and measured to evaluate the level of inflammatory cyto-chemokines, whereas cell pellet subjected to FACS analysis. CountBright™ Absolute Counting Beads (Thermofisher, Rugby, UK) were added to 300 μl of resuspended cells, and samples were analysed by flow cytometry gating separately on beads and cells as previously described [28].

2.12. Cytokines and chemokines protein array

Equal volumes (1.5 ml) of pouch inflammatory fluids in all experimental conditions were incubated with the precoated proteome profiler array membranes according to the manufacturer's instructions. Dot plots were detected by using the enhanced chemiluminescence detection kit and Image Quant 400 GE Healthcare software (GE Healthcare, Italy) and successively quantified using GS 800 imaging densitometer software (Biorad, Italy) as previously described [29].

2.13. Transwell chemotaxis assay

Chemotaxis was assessed using a transwell assay. Gal-9 (1–30 nM) and C-X-C Motif Chemokine Ligand 12 (CXCL-12) (6448-SD,RD USA; 10 μg/ml) alone or in combination (final volume 700 μl) in M199 media were added to the bottom well of a Transwell-24 permeable support with 3.0 μm pores (Corning, NY, USA). 2×10^5 T cells in a final volume of 200 μl were to the top chamber which had a confluenent HDBEC monolayer activated with TNF-α (100 U/ml) and IFN-γ (10 ng/ml) for 24 h. After 2 h at 37 °C T cells were collected from the bottom wells and quantified by flow cytometry using CountBright™ Absolute Counting Beads (Thermofisher, Rugby, UK) as previously described [12,20].

2.14. Solid-phase binding assay

The direct solid-phase binding assays were carried out according to previously documented protocol [30,31]. Briefly, 96-well microplates (Fisher Scientific) were coated in the presence of 10 nM Gal-9 overnight at 4ºC, respectively. After blocking with BSA, an increasing concentration series (0–1000 nM) of recombinant human CXCL12-Fc construct (10118-H01H, Sino Biological) was added into the Gal-9 isoform coated wells. The binding of CXCL12-Fc to immobilised Gal-9 isoforms was detected by HRP-conjugated anti-human IgG antibody (62–8420, Invitrogen) followed by addition of 3, 3′, 5, 5′-tetramethylbenzidine liquid substrate (T444, Sigma-Aldrich). Each incubation was followed by washing steps and colour development of the substrate was stopped by 1 M H_2SO_4. Absorbance at the wavelength of 450 nm was measured with a SpectraMax Microplate Reader (Molecular Devices).

2.15. Statistical analysis

Data are presented as mean ± SEM. Multiple group comparisons

were made using one-way or two-way ANOVA followed by Dunnett's or Bonferroni's *post hoc* analysis. Where two conditions were compared using a Student's t test. $p < 0.05$ was considered significant. Four-parameter non-linear regression analysis with variable slopes was utilised to generate logarithmic concentration-binding curves. All statistics were analysed on Prism version 8.0.2 (GraphPad Software).

3. Results

3.1. Endogenous Gal-9 is expressed in T cell subsets

Accumulative evidence indicates divergent physiological roles for Gal-9, however, studies exploring its endogenous expression profile in T cells subsets remain lacking. We therefore initially examined the endogenous expression of Gal-9 in T cell subsets. Extracellular staining revealed a low level of Gal-9 expression on both $CD4^+$ and $CD8^+$ T cells compared to the isotype control (Fig. 1Ai). Gal-9 labelling following cellular permeablisation revealed a much more significant increase in the total expression of Gal-9, indicating a predominant intracellular pool of endogenous Gal-9 protein expression in both T cell subsets (Fig. 1Ai-ii).

3.2. Soluble Gal-9 binds $CD4^+$ and $CD8^+$ subsets in a glycan dependent manner

We next sought to investigate the binding capacity of exogenous Gal-9 to the surface of T cell subsets using flow cytometry. A significant increase in Gal-9 binding to $CD4^+$ and $CD8^+$ T cells was observed following incubation with several concentrations of soluble Gal-9 in comparison to untreated cells (Fig. 1Bi & ii & Supplementary Figure 1Ai-ii & Bi-ii). Gal-9 is known to bind to both glycoproteins and glycolipids containing a varying degree of oligosaccharide modifications in a highly specific manner [32]. To determine if the binding of Gal-9 to T cells was carbohydrate-dependent, we used lactose (which contains L-galactose which is the preferential ligand for Gal-9) as a pan-galectin antagonist. Isolated $CD4^+$ and $CD8^+$ cells were incubated with 25 mM lactose first and then 100 nM Gal-9 or vice versa. Flow cytometry analysis showed that, in the presence of lactose, the binding of Gal-9 was significantly reduced to both $CD4^+$ (Fig. 1 C) and $CD8^+$ (Fig. 1D) T cells but not fully abolished. Inhibition was observed either when lactose was added before or after incubation with Gal-9. The gating strategy utilised for flow cytometry is presented in (Supplementary Figure 2Ai-v). Collectively these data suggest that the interaction between exogenous Gal-9 and $CD4^+$ and $CD8^+$ T cells in part, was indeed glycan dependent.

3.3. Exogenous Gal-9 supports $CD4^+$ and $CD8^+$ T cell adhesion and transmigration

Given the ability of Gal-9 to bind both $CD4^+$ and $CD8^+$ T cells, we assessed whether Gal-9 could promote T cell adhesion and transmigration. To address this, we performed a static adhesion assay, where T cells were incubated with Gal-9 for 20 min at RT before being added to activated HDBEC. Representative images (shown in Figure 2Ai-ii) and quantification illustrated that treatment with soluble Gal-9 increased the proportion of adherent and phase-dark transmigrated (Fig. 2B-C) $CD4^+$ and $CD8^+$ T cells in a dose dependent manner. Similar adhesion/migration effects were observed when HDBECs were treated with Gal-9 prior to the addition of $CD4^+$ or $CD8^+$ T cells (Supplementary Figure 3Ai-ii). These data indicate that soluble Gal-9 facilitates the adhesion and transmigration of $CD4^+$ and $CD8^+$ T cells on activated endothelium.

3.4. Gal-9 induces L-selectin shedding and upregulates LFA-1 and CXCR4 expression

To further validate the contribution of Gal-9 to T cell adhesion/migration, we measured the expression of several adhesion and chemokine receptors, L-selectin, LFA-1 and CXCR4, on both $CD4^+$ and $CD8^+$ T cells following stimulation with soluble Gal-9 (Figure 3Ci-iii). We found that Gal-9 (10–100 nM) significantly induced L-selectin shedding (Figure 3Ai-Bi) and increased the expression of LFA-1 (Figure 3Aii-Bii) and CXCR4 (Figure 3Aiii-Biii) in a dose dependent manner compared to untreated controls. Fig 3.

3.5. Gal-9 promotes the expression of adhesion molecules on endothelial cells

We next sought to establish if Gal-9 alone or in combination with other inflammatory mediators could upregulate adhesion molecule expression on HDBEC. Our results showed that Gal-9 alone did not significantly upregulate the expression of ICAM-1 (Fig. 4 Ai) or VCAM-1 (Figure 4Bi) on HDBEC. However, in combination with other proinflammatory stimuli (TNF-α and IFN-γ), ICAM-1 and VCAM-1 expression was significantly increased compared to TNF-α/IFN-γ group (Fig. 4A-B). The gating strategy utilised for flow cytometry is presented in (Supplementary Figure 4Ai-ii). To determine whether endothelial derived Gal-9 had a functional impact on T cell migration, we used siRNA to knock down endogenous Gal-9 expression in HDBEC and performed a migration assay with $CD4^+$ T cells. The knockdown (~50%) was confirmed with flow cytometry (Figure 4 Ci). Representative images (Figure 4Cii-iii) and quantification (Figure 4Civ) showed that $CD4^+$ T cell adhesion and transmigration was reduced in Gal-9 siRNA treated HDBECs compared to scrambled control (Figure 4Cii-iv).

3.6. Gal-9 supports T cell capture in a glycan and integrin dependent manner

Shear stress in one of the predominant stimuli for ECs and can dictate the expression of adhesion molecules which ultimately influences the binding of leukocytes to the surface of the endothelium [33]. To investigate the extent of T cell adhesion to Gal-9 under physiological flow conditions, we performed flow-based adhesion assays by perfusing isolated $CD4^+$ and $CD8^+$ T cell suspensions through chambers coated with different concentrations of Gal-9 (Fig. 5 A). Our results showed that immobilised Gal-9 could indeed support direct capture and adhesion of $CD4^+$ and $CD8^+$ T cells under physiological flow (0.05 Pa) in a dose dependent manner (Figure 5Bi). We also corroborated our previous results in the static migration assay and showed that pre-incubation of immobilised Gal-9 with lactose for 20 min at RT significantly inhibited adhesion of both $CD4^+$ and $CD8^+$ T cells under flow (Figure 5Bii). Collectively these data confirmed that the binding of Gal-9 to $CD4^+$ and $CD8^+$ T cells was glycan dependent, under both static and flow conditions. Considering the ability of Gal-9 to induce integrin activation, we next investigated whether adhesion to immobilised Gal-9 under flow was integrin dependent. Our results showed that pre-incubation of T cells with a CD18 neutralising antibody significantly reduced both $CD4^+$ and $CD8^+$ T cell adhesion (Figure 5Biii), confirming an integrin dependent mechanism was involved. To confirm that these effects were truly Gal-9 specific, we also utilised soluble recombinant human Tim-3-Fc construct as a competitive inhibitor. We found that the pre-incubation of immobilised Gal-9 with soluble Tim-3-Fc completely blocked the capture and adhesion of perfused T cells to Gal-9 coated surfaces, demonstrating Gal-9 specificity (Supplementary Figure 5Ai-ii).

3.7. Gal-$9^{-/-}$ mice display impaired leukocyte trafficking

To further corroborate the role of endogenous Gal-9 in leukocyte recruitment *in vivo* we utilised the dorsal air-pouch with zymosan in Gal-9 knockout (Gal-$9^{-/-}$) mice. As shown in Fig. 6 A, 24 h after a single injection of 0.5 mg zymosan, leukocyte recruitment was significantly reduced into the air-pouch of Gal-$9^{-/-}$ mice compared to WT controls (Figure 6Aii). To gain some insights into other possible differences in the

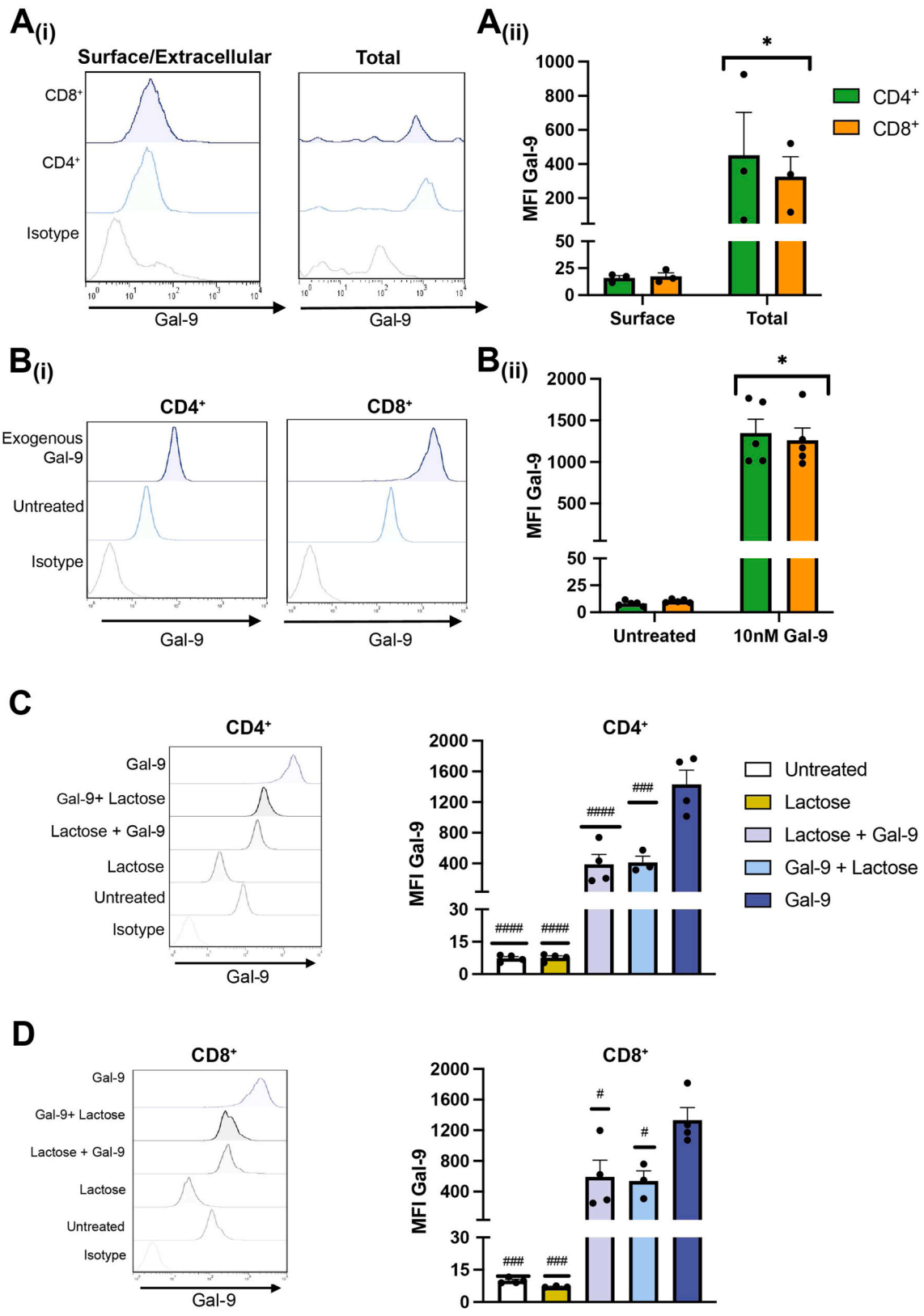

Fig. 1. Soluble Gal-9 binds $CD4^+$ and $CD8^+$ subsets in a glycan dependent manner. PBMCs were separated in both $CD4^+$ and $CD8^+$ T cell subsets and flow cytometric analysis was performed to measure extracellular and total Gal-9 protein levels expressed as median fluorescence intensity (MFI) (Ai-ii). Moreover, isolated $CD4^+$ and $CD8^+$ were incubated with 100 nM Gal-9 for 20 min to quantify the binding capacity of exogenous Gal-9 to the surface of T cell subsets using flow cytometry (expressed as MFI) (Bi-ii). Isolated $CD4^+$ (C) and $CD8^+$ (D) were incubated first with 25 mM lactose and then with 100 nM Gal-9 or vice versa. Flow cytometry analysis was used to quantify the Gal-9 protein level with or without Lactose inhibition (expressed as MIF) (C-D). Ordinary one-way ANOVA (B, C) or two-way ANOVA (A, B) followed by post-hoc Tukey test was used as a parametric test. *$p < 0.05$, Surface with Total group and Untreated group with 100 nM Gal-9 group; #$p < 0.05$, ###$p < 0.001$, ####$p < 0.0001$, compared to Gal-9 group. Data are expressed as mean ± standard error of mean (SEM). ($n = 3$).

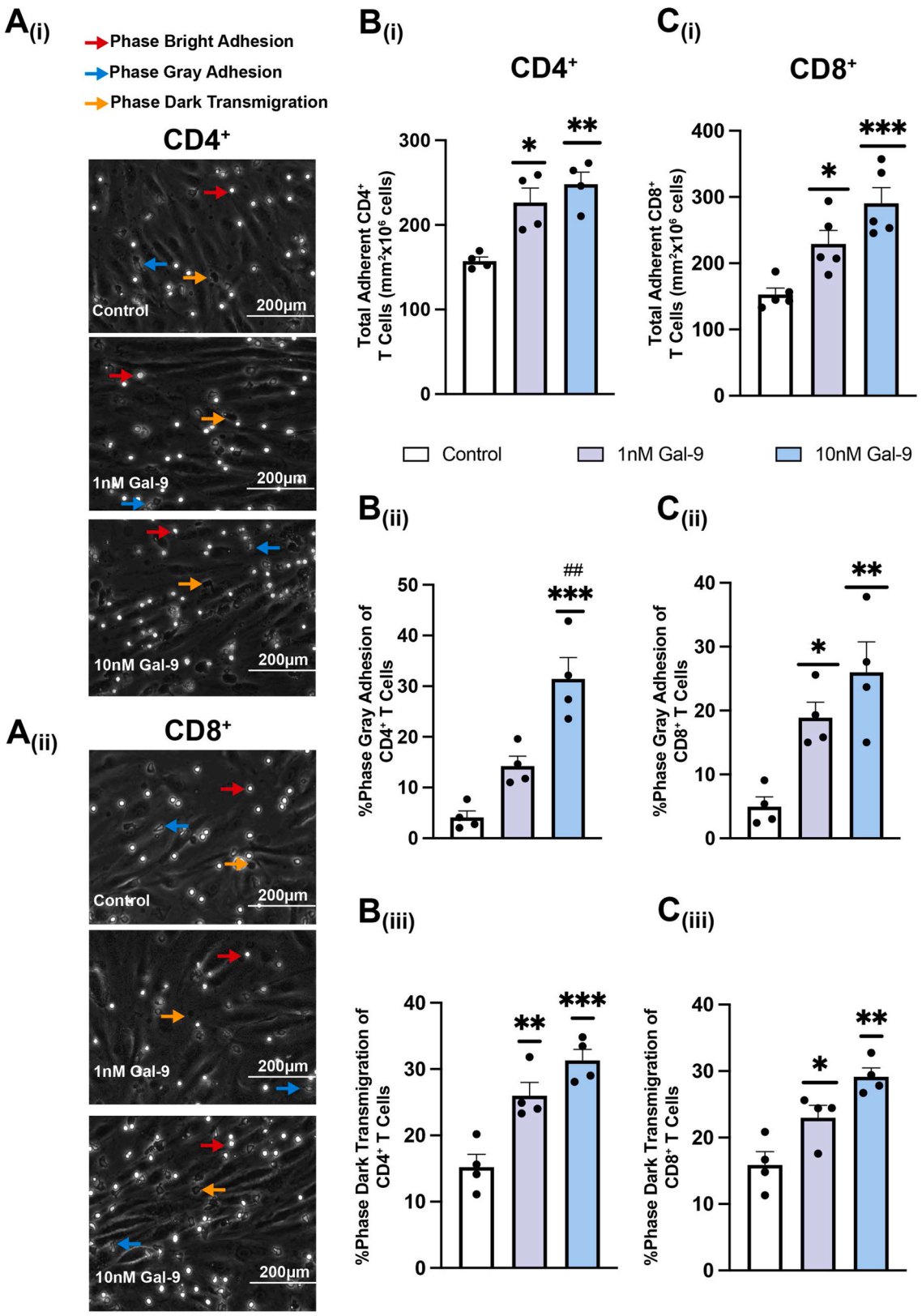

Fig. 2. Gal-9 promotes $CD4^+$ and $CD8^+$ T cell adhesion and transmigration. Human dermal blood endothelial cells (HDBECs) were stimulated with TNF-α (100 U/ml) and IFN-γ (10 ng/ml) for 24 h. $CD4^+$ and $CD8^+$ T cell subsets were incubated with or without Gal-9 (1–10 nM) for 20 min at 37 °C. In the panel Ai and ii representative images of respectively $CD4^+$ and $CD8^+$ T cell adhesion (indicated as phase bright and spherical in morphology or as dark grey and ruffled plasma membrane) and transmigration (indicated as black and elongated morphology) are shown. Quantification of $CD4^+$ and $CD8^+$ total adhesion (Bi and Ci), % of adhesion (Bii and Cii) and % of transmigration (Biii and Ciii) was performed using Image-pro 6.0 software. Ordinary one-way ANOVA followed by post-hoc Tukey test was used as a parametric test. *$p < 0.05$, * *$p < 0.01$, * **$p < 0.001$, compared to Control group; ##$p < 0.01$, compared to 1 nM Gal-9 group. Data are expressed as mean ± standard error of mean (SEM). (n = 4–5).

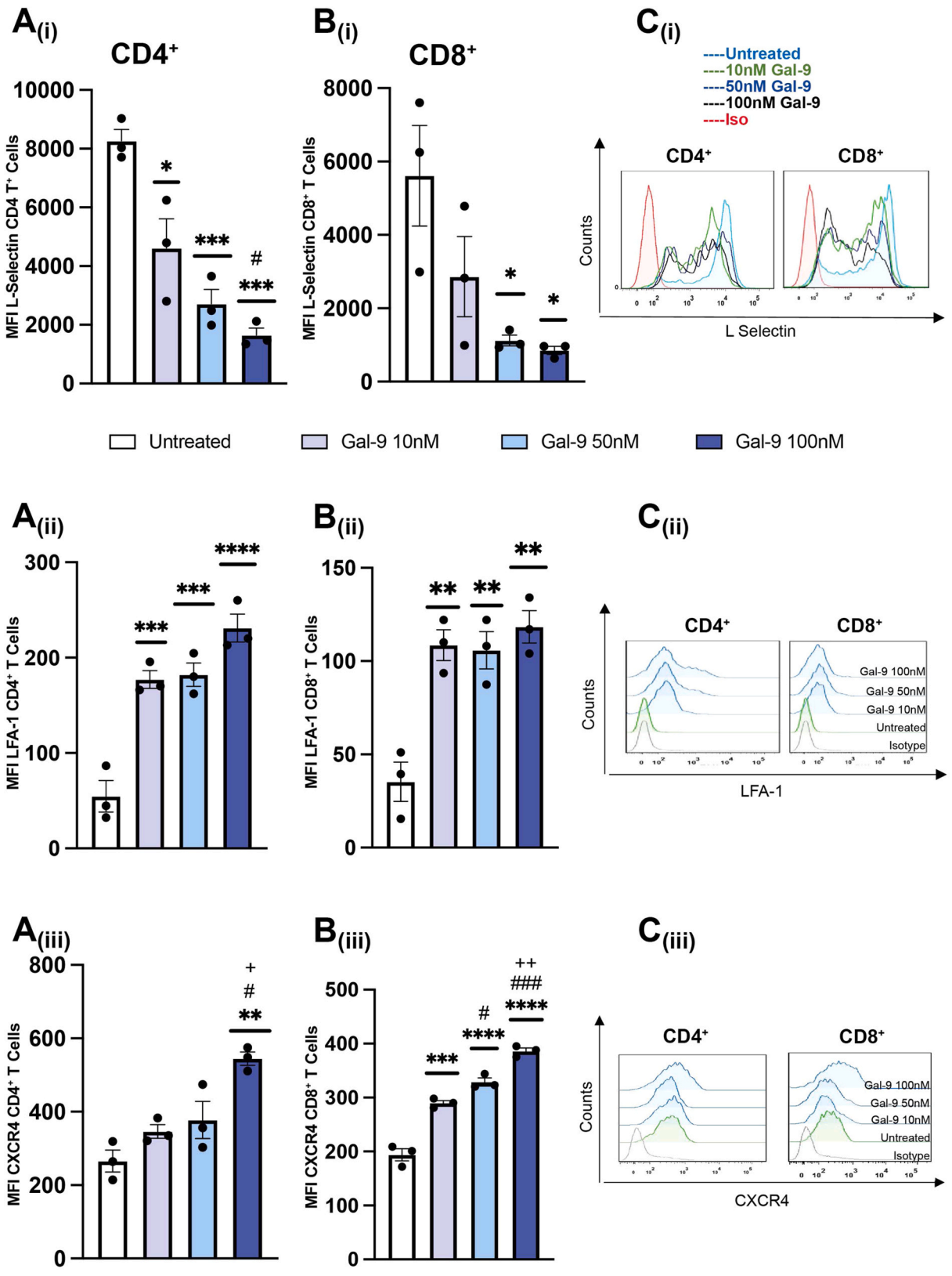

Fig. 3. Gal-9 induces L-selectin shedding, and upregulates LFA-1 and CXCR4 expression. Isolated $CD4^+$ and $CD8^+$ were incubated with or without Gal-9 protein (10, 50 and 100 nM). Flow cytometry analysis was used to quantify (respectively for CD4 and CD8) L-selectin (Ai and Bi), LFA-1 (Aii and Bii) and CXCR4 (Aiii and Biii) protein level (expressed as MIF). Facs images represent L-selectin, integrin and CXCR4 shift compared to the isotype control in both CD4 and CD8 T cells (Ci-iii). Ordinary one-way ANOVA followed by post-hoc Tukey test was used as a parametric test. *$p < 0.05$, * *$p < 0.01$, * **$p < 0.001$, * ** *$p < 0.001$ compared to Untreated group; #$p < 0.05$, ###$p < 0.001$, compared to Gal-9 10 nM group; +$p < 0.05$, + +$p < 0.01$, compared to Gal-9 50 nM group. Data are expressed as mean ± standard error of mean (SEM). (n = 3).

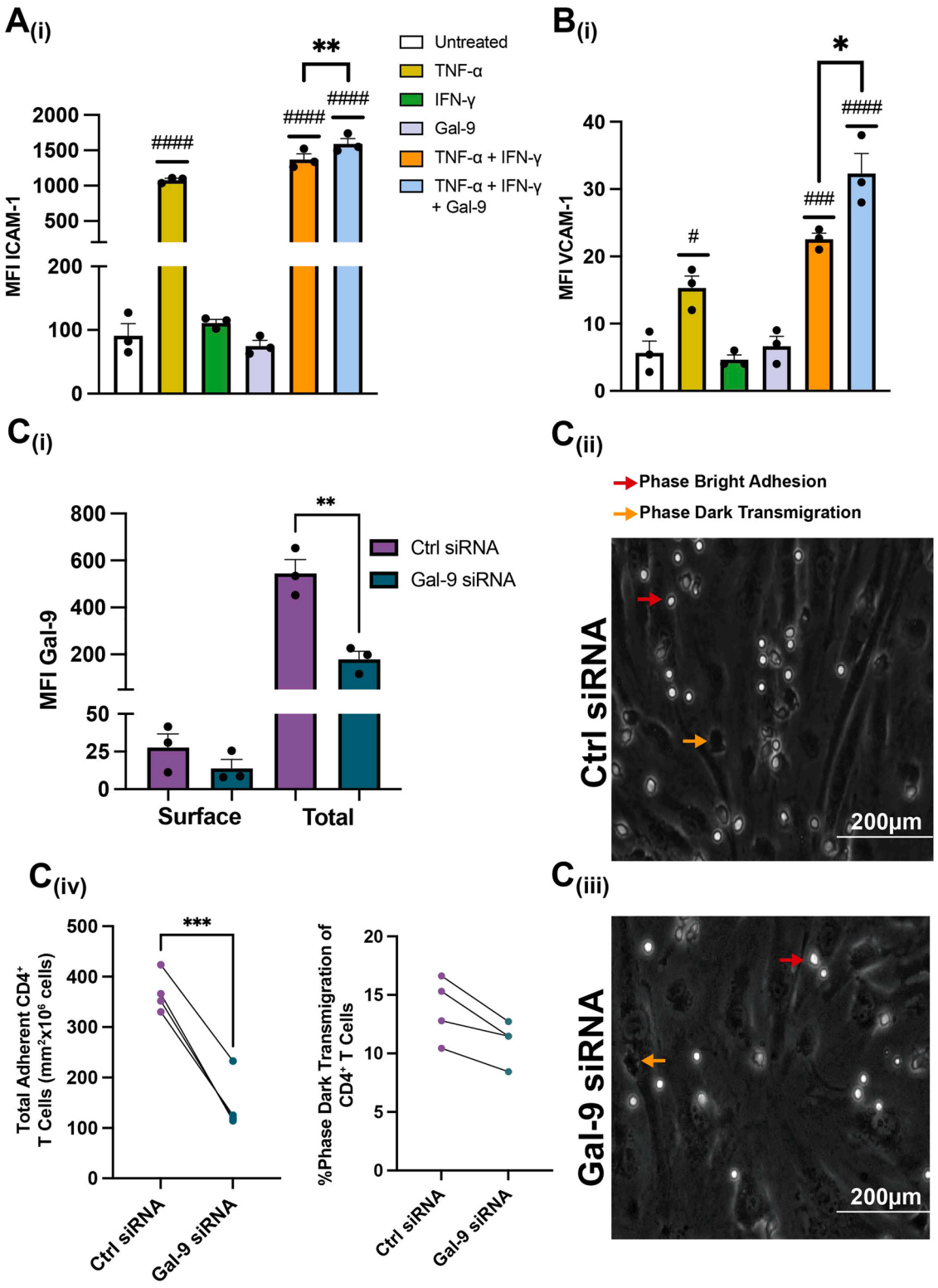

Fig. 4. Impaired T cell adhesion and transmigration following knockdown of endogenous Gal-9. Human dermal blood endothelial cells (HDBECs) were stimulated with TNF-α (100 U/ml) and IFN-γ (10 ng/ml) alone or in combination with Gal-9 for 24 h. Cells were washed, gated in their totality and singlet before the identification of ICAM (Ai) and VCAM (Bi) expression. Histograms values (expressed as MIF) indicate the total positive cells, in the different experimental conditions (Ai and Bi). Flow cytometric analysis of surface (extracellular) and total Gal-9 expression by stimulated ECs (with TNF-α and IFN-γ) was evaluated after transfection with Gal-9 or control SiRNA (Ci). Representative images for respectively Ctrl siRNA (Cii) and Gal-9 siRNA (Ciii) are represented to analyse T cell adhesion (indicated as phase bright and spherical in morphology) and transmigration (indicated as black and elongated morphology). Quantification of Ctrl siRNA and Gal-9 siRNA total adhesion and % of transmigration was performed using Image-pro 6.0 software (Civ). Unpaired t-test (B, C) or ordinary one-way ANOVA (A) followed by post-hoc Tukey test was used as a parametric test. *$p < 0.05$, * *$p < 0.01$, * **$p < 0.001$; #$p < 0.05$, ###$p < 0.001$, ####$p < 0.0001$, compared to Untreated group. Data are expressed as mean ± standard error of mean (SEM). (n = 3–4).

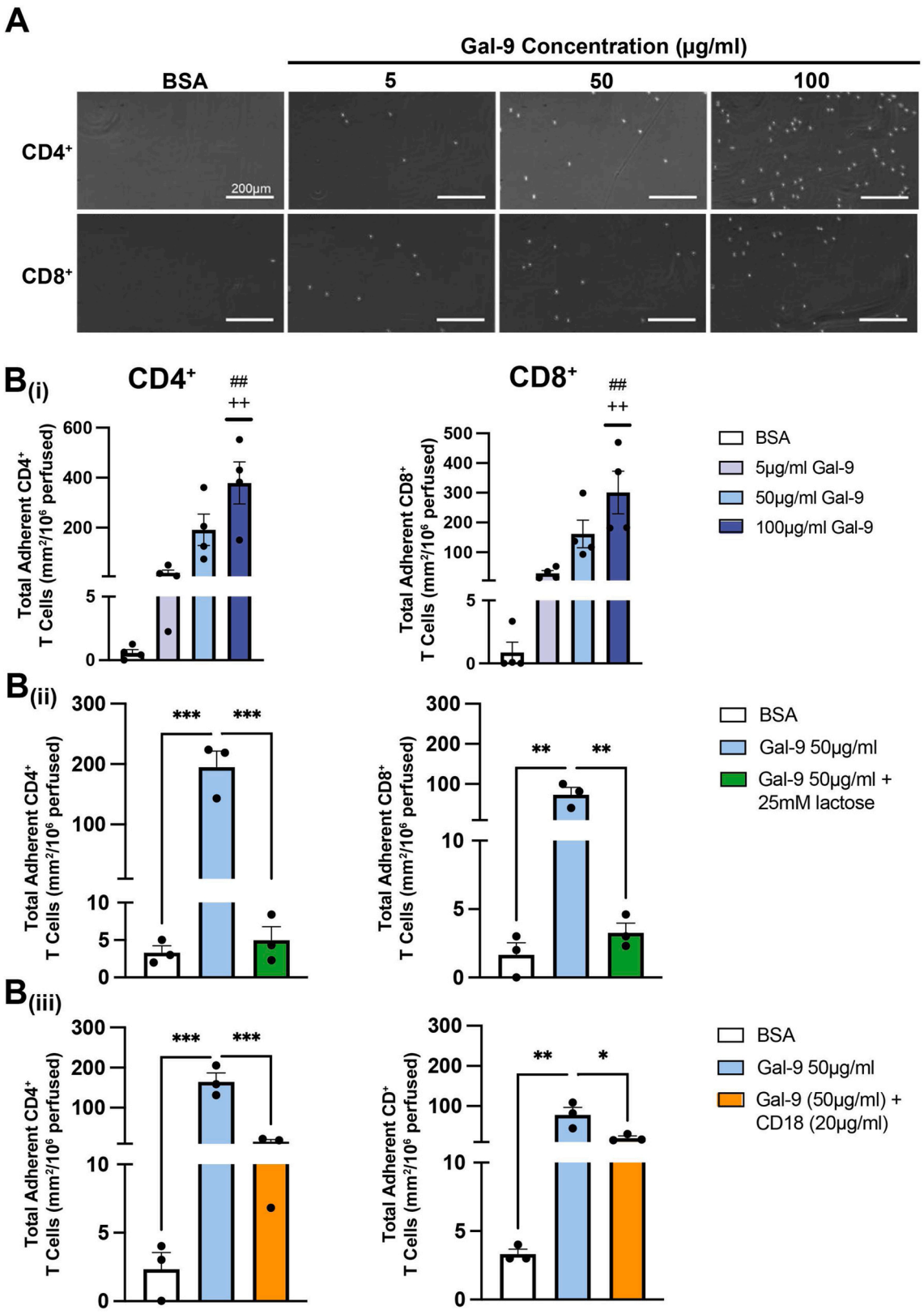

Fig. 5. Gal-9 supports the recruitment of T cell subsets under physiological flow. Representative images of the centre of ibidi channels on isolated $CD4^+$ and $CD8^+$ cells were flown over immobilized Gal-9 (0–100 μg/ml) protein (A). In the panel Bi is shown the quantification of the total $CD4^+$ and $CD8^+$ adhesion cells based on seven images taken across the centre of each channel. $CD4^+$ and $CD8^+$ were pre-incubated with or without 25 mM lactose (Bii) or 20 μg/ml CD18 antibody (Biii) prior to being flowed over the immobilised Gal-9 at a wall shear stress of 0.05 Pa for 4 min. Quantification of adherent cells was performed with Image-pro 6.0 software. Ordinary one-way ANOVA (B, C, D) followed by post-hoc Tukey test was used as a parametric test. *$p < 0.05$, * *$p < 0.01$, * **$p < 0.001$; ##$p < 0.01$, compared to BSA group; + +$p < 0.01$, compared to 5 μg/ml Gal-9 group. Data are expressed as mean ± standard error of mean (SEM). (n = 3).

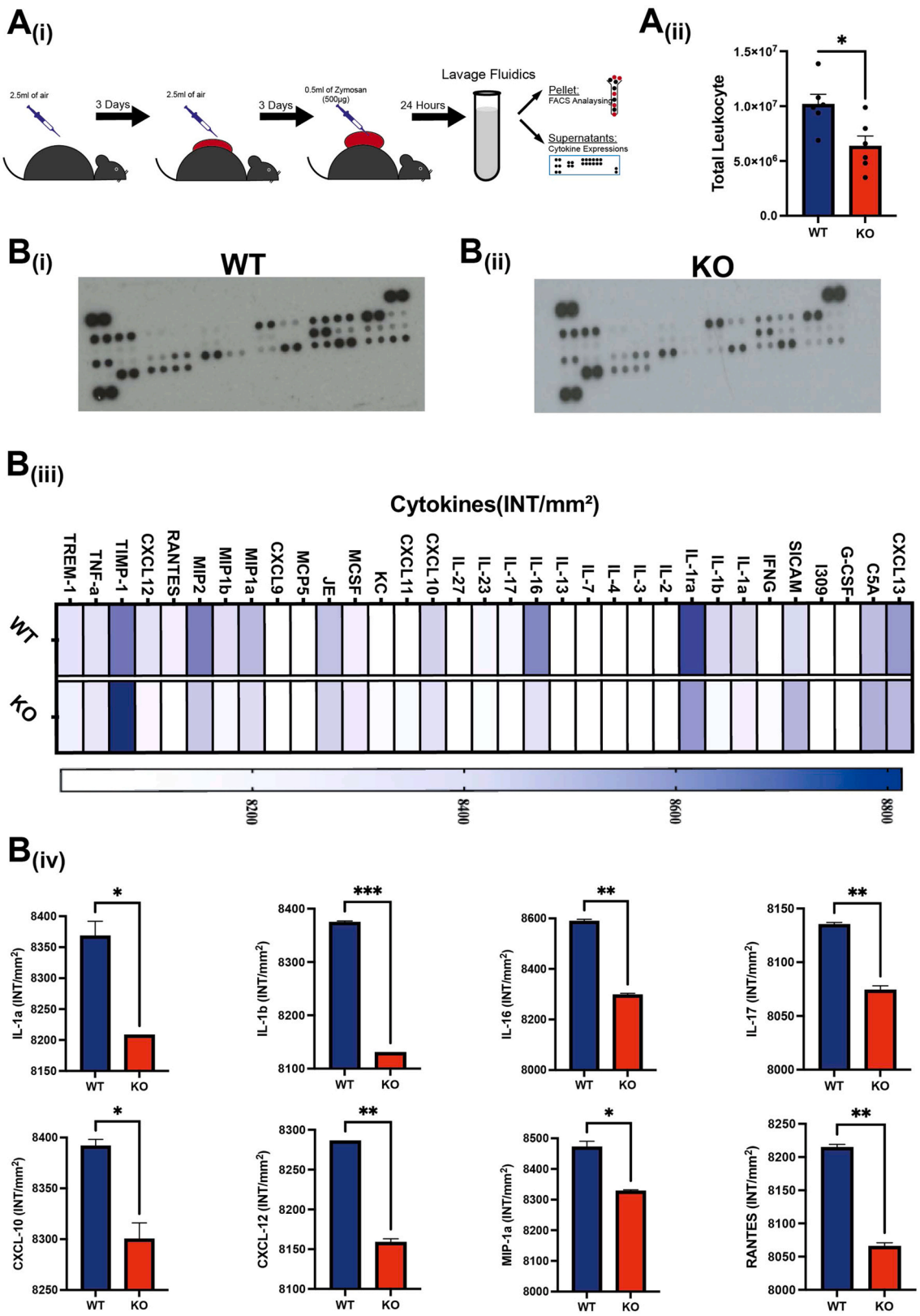

Fig. 6. Gal-9KO mice display impaired leukocyte trafficking. Representative scheme of *in vivo* model of the air pouch and subsequent *ex vivo* analyses are presented in the panel Ai. Total cell number from pouches inflammatory exudates in both WT and Gal-9KO was evaluated at 24 h (Aii). Inflammatory supernatants obtained from the pouch cavities were assayed using a Proteome Profiler cytokine array for WT (Bi), and Gal-9KO (Bii). Densitometric analysis is presented as heatmap (Biii). Thereafter, IL-1α, IL-1β, IL-16, IL-17,CXCL-10, CXCL-12, MIP-1α, and RANTES were extrapolated from heatmap and represented graphically (Biv). Data (expressed as INT/mm^2) are presented as means ± standard error of mean (SEM) of positive spots of three separate independent experiments run each with n = 6 mice per group pooled. Statistical analysis was conducted by unpaired t-test as a parametric test. *$p < 0.05$, * *$p < 0.01$, * **$p < 0.001$, compared to WT group.

inflammatory response caused by zymosan stimulus, we used an unbiased approach (pre-made protein array) to profile cyto-chemokines present in the inflammatory fluids. As shown in Fig. 6B, the pouch fluid obtained from WT mice treated with zymosan (Figure 6Bi) showed a large increase in pro-inflammatory mediators compared to Gal-9$^{-/-}$ mice (Figure 6Bii). Densitometric analysis, (extrapolated from the heat maps Figure 6Biii), revealed that the WT treated group had a specific up-regulation in the following factors: Interleukin (IL)− 1α, IL-1β, IL-16, IL-17, CXCL-10, CXCL12, Macrophage Inflammatory Protein-1 Alpha (MIP-1α), and regulated upon activation, normal T Cell expressed and presumably secreted (RANTES), compared to the Gal-9$^{-/-}$ group (Figure 6Biv).

3.8. Gal-9 selectively binds CXCL12 and inhibits its chemotactic function

Recent evidence suggests that galectins may obstruct chemokine binding to their cognate receptors and produce inhibitory effects on chemotaxis [12]. Considering the strong correlation between the absence of Gal-9 and increased circulating levels of the chemokine CXCL12 in our previous *in vivo* results (Figure 6Biv), we hypothesised that Gal-9 potentially acts in a similar manner. Initially we examined whether Gal-9 could interact with CXCL12 *via* a solid phase binding assay. In support of this hypothesis, we observed that Gal-9 exhibited a strong binding affinity for rhCXCL12 with a half maximal effective concentration (EC_{50}) of ~20 nM (Fig. 7 A). We went on to perform a transwell chemotaxis assay, and found that Gal-9 had no chemotactic effects *per se*. However, when co-incubated with CXCL12 in the bottom well, chemotaxis was significantly inhibited (Fig. 7B). This inhibition was only observed when Gal-9 was added to the bottom wells of the plate with CXCL12 suggesting that Gal-9 can inhibit and/or override the effects of this chemokine through specific binding.

4. Discussion

In the present study, we have demonstrated novel functions for Gal-9 as an accessory molecule that supports capture, firm adhesion, and migration of CD4$^+$/CD8$^+$ T cells under both static and physiological flow conditions. Previous reports have shown Gal-9 to be widely distributed in various tissues and cells, including thymus, ECs, fibroblasts, and immune cells such as neutrophils, monocytes, and dendritic cells [34]. CD4$^+$ T cells were reported to secret Gal-9 in a soluble form [35]. Circulating CD4$^+$ and CD8$^+$ T cells, and tumour-infiltrating T cells exhibit high surface expression of Gal-9 in patients with virus-associated solid tumours [36]. However, to our knowledge, cellular expression in resting T cells has not been previously reported. We report, for the first time, similar extracellular and intracellular pools of Gal-9 in both primary CD4$^+$ and CD8$^+$ T cells as assessed by flow cytometry. Interestingly, intracellular/total Gal-9 levels were significantly higher compared to extracellular/surface level in both T cell subsets. We further studied the interaction of exogenous Gal-9 with T cell subsets to dissect the specificity of binding characteristics. We showed an increase in extracellular binding following incubation of T cells with Gal-9 (10–100 nM). Soluble Gal-9 has been reported to act in an autocrine fashion on peripheral CD4$^+$ T cells, inducing IFN-γ secretion, apoptosis, T cell activation and proliferation in a Lck-kinase dependent manner as observed with canonical CD3 activation [22,37]. As IFN-γ is also an inducer of Gal-9 expression and T cell activation can alter surface receptor expression, the increase in binding could also be the result of a positive feedback loop, with Gal-9 further amplifying its own endogenous expression and up-regulation of known receptors (*e.g.* Tim-3, CD44) on CD4$^+$ T cells [38].

A study from Bi et al., proposed that Gal-9 interacts with extracellular protein disulfide isomerase (PDI) on murine Th2 cells, CEM, Jurkat and PhaRST6 T cells and promotes β3 integrin-mediated murine Th2 cell migration [39]. However, whether Gal-9 induces adhesion and transmigration of primary human T cells remained unclear. Here we have

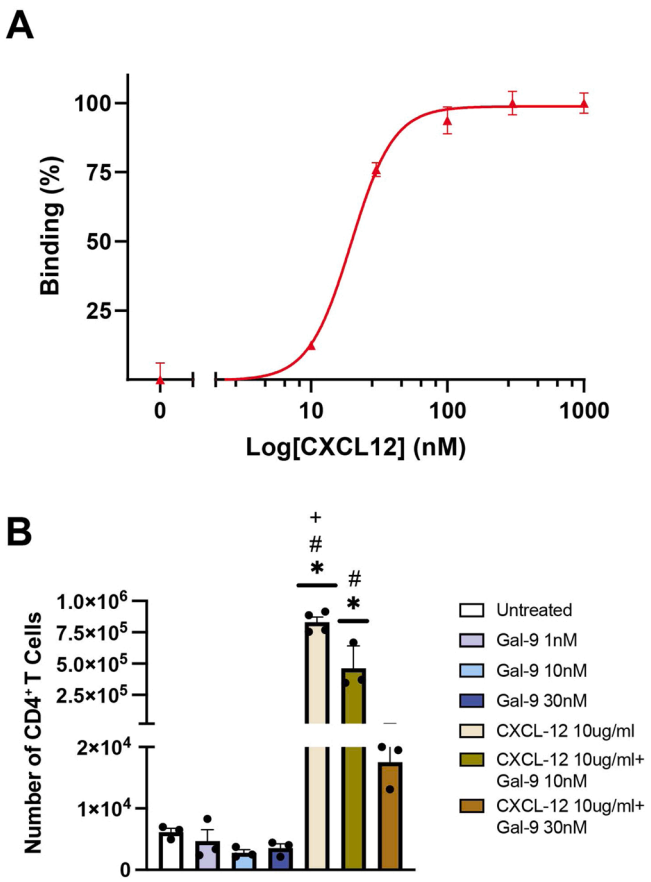

Fig. 7. Gal-9 selectively binds CXCL12 and inhibits chemotactic activity. (A) The concentration-binding curve of rhCXCL12 ($EC_{50} \approx 20$ nM) to immobilised Gal-9 (coated in the presence of 10 nM Gal-9). (B) CD4$^+$ cells were seeded into the top chamber which had a confluent HDBEC monolayer activated with TNF-α (100 U/ml) and IFN-γ (10 ng/ml) for 24 h. The cells migration after Gal-9 (1–30 nM) alone or in combination with CXCL12 (10 μg/ml) treatment was quantified using CountBright™ Absolute Counting Beads. Ordinary one-way ANOVA (A) followed by post-hoc Tukey test was used as a parametric test. *$p < 0.05$, compared Untreated, Gal-9null 1 nM, Gal-9null 10 nM and Gal-9null 30 nM to other groups; $^{\#}p < 0.05$, compared CXCL-12 10 ug/ml+ 30 nM Gal-9 group to CXCL-12 10 ug/ml and CXCL-12 10 ug/ml+ 10 nM Gal-9; $^{+}p < 0.05$, compared CXCL-12 10 ug/ml+ 10 nM Gal-9 to CXCL-12 10 ug/ml. Data are expressed as mean ± standard error of mean (SEM). (n = 3).

shown that pre-treatment of both primary CD4$^+$ and CD8$^+$ T cells with soluble Gal-9 supports adhesion and transmigration through activated EC monolayer under static conditions *in vitro*. To further confirm that Gal-9 contributes to T cell migration, expression levels of L-selectin (adhesion molecule that regulates the trafficking of leukocytes[40]), LFA-1 (integrin involved in adhesion, extravasation, and migration [41]), and CXCR4 (chemokine receptor constitutively expressed and regulates T cell chemotaxis [42]) on CD4$^+$ and CD8$^+$ T cells were examined. We found that stimulation with soluble Gal-9 induced LFA-1 and CXCR4 upregulation and L-selectin shedding in both T cell subsets.

Recent findings attribute an endothelial-specific function of several galectins [1]. Transmigration of modified T lymphocyte cell lines through stimulated human umbilical vein endothelial cells (HUVECs) was significantly inhibited by Gal-1 compared to unstimulated HUVECs [43]. More recently a study reported Gal-3 binding mediates the interaction between leukocytes and CXCL-12 on ECs [12]. Yamamoto et al., reported increased binding of B cells, neutrophils, eosinophils and monocytes to HUVECs following pre-incubation with increasing concentrations of Gal-8 and − 9 [17]. Here, we show that pre-treatment of CD4$^+$ and CD8$^+$ T cells or the endothelium itself with Gal-9 promotes

adhesion and transmigration.

Interestingly, immobilised Gal-9 did not induce rolling, rather instant capture and firm adhesion of T cell subsets, which is a similar behaviour we observed previously with neutrophils and monocytes [20,44]. Since rolling is dependent upon selectin expression, it is quite possible that Gal-9 may be behaving as surrogate selectin, thereby modulating binding affinity to the T cell expressed selectins [45]. Another tandem repeat member of the galectin family, Gal-8 has been reported to have pro-adhesive behaviour on neutrophils *via* interaction with alphaM (MAC-1) and in Jurkat T Cells *via* interaction with alpha4 (VLA-4) integrins [17,46]. In the same study the authors showed a similar interaction with Gal-9 and Jurkat T Cells in the context of adhesion, suggesting that leukocyte-tandem repeat type galectin interactions may bypass rolling to achieve direct integrin-mediated adhesion. Interestingly, immobilized Gal-1 did not promote capture or adhesion with $CD4^+$ and $CD8^+$ T cells in flow-based assays further highlighting this specific function of Gal-9 (data not shown).

Blocking studies with lactose and CD18 antibody indicates that the adhesion to Gal-9 is glycan and β2 integrin-dependent. Intriguingly, immobilised Gal-9 also failed to capture $CD4^+$ and $CD8^+$ T cells after incubation with soluble recombinant Tim-3-Fc, suggesting potential competition between the recombinant Tim-3 and CD18 on T cells. While it was previously argued by some that the interaction between Gal-9 and Tim-3 was not observed in cell-based and solid-phase binding assays, many more studies have generated convincing evidence to suggest that the binding of Gal-9 to Tim-3 does indeed occur in T cells [24,47,48]. Our results further corroborated this interaction and moreover indicate that the binding site of Tim-3 on Gal-9 may potentially overlap with that of CD18.

To study the endogenous functions of galectins *in vivo*, studies in transgenic mice have been essential. Gal-1 appears to exhibit anti-inflammatory functions, with increased extravasation observed into inflamed cremaster of Gal-$1^{-/-}$ compared to WT [11]. Gal-3, on the other hand, has been shown to promote leukocyte recruitment *in vivo*, with altered slow rolling and emigration of leukocytes in Gal-$3^{-/-}$ mice [13]. Interestingly, isolated Gal-$3^{-/-}$ mouse ECs showed reduced surface expression of ICAM-1 and E-selectin post stimulation with IL-1β compared to WT, suggesting that endothelial function may be impaired in the absence of endogenous Gal-3 [13]. There is limited experimental evidence relating to the role of endogenous Gal-8 and − 9 on leukocyte trafficking *in vivo*. Despite these compelling reports, an endothelial-specific galectin knockout mouse model is needed to explore and understand the mechanistic and regulatory pathways of galectin function. Considering that there is growing evidence that indicates elevated levels of Gal-9 in the serum of patients with chronic inflammatory conditions [49,50], we used a well-established preclinical model of acute inflammation, the dorsal air pouch [27]. We tested the hypothesis that in the absence of endogenous Gal-9 a reduction in leukocyte recruitment and inflammatory mediator generation would be observed. Indeed, we found that zymosan administration into the air-pouch of Gal-$9^{-/-}$ mice evoked a reduced leukocyte infiltrate and pro-inflammatory mediator production compared to WT.

Interestingly several chemokines including CXCL12, CCL5 and CXCL9 were significantly reduced in Gal$9^{-/-}$ mice. It is well established that chemokines and galectins regulate leukocyte recruitment and can be simultaneously upregulated under inflammatory conditions [51]. Due to the functional and structural similarities between chemokines and galectins, it has been hypothesised and demonstrated that members of both effector molecule families can form chemokine/galectin heterodimers with functional consequences [12,52]. Since CXCL12 and other galectins (*e.g.* Gal-3) have been shown to be simultaneously upregulated under chronic inflammatory conditions, we tested and demonstrated that Gal-9 could specifically block CXCL12-induced T cell chemotaxis by directly binding and interfering with its activity. Given our finding that Gal-9 is a potential CXCL12 antagonist, the current evidence for chemokine/galectin heterodimerization will require further investigation into the interactome and its pathophysiological relevance. The interaction of a lectin with a non-glycan counter-receptor could potentially be exploited for therapeutic application [53].

5. Conclusion

In conclusion, our study characterises, for the first time, the capture, adhesion, and migration behaviour of $CD4^+$ and $CD8^+$ T cells to immobilised Gal-9 and/or endothelial-derived/presented Gal-9, under static and physiological flow conditions. We further demonstrate differential binding characteristics of Gal-9 to T cell subtypes, which could be of potential therapeutic significance, specifically in the treatment of autoimmune diseases, given the ability of Gal-9 to promote apoptosis in pathogenic T cells subsets.

Funding

AAM is supported by a King Khalid University funded scholarship (57875). FR is supported by a University of Naples Federico II PhD scholarship in Pharmaceutical Sciences. AS is supported by a Dompé Farmaceutici S.p.A fellowship for PhD programme in "Nutraceuticals, functional foods and human health" (University of Naples Federico II). AJI is supported by a Birmingham Fellowship.

Author Contributions

AAM, FR, MS, AS, JB, ZZ, LP and ST performed experiments. AAM, FR, MS, FM and AJI analysed results and made the figures. AJI and FM designed the research. AAM, FR, FM, and AJI wrote the paper. All authors contributed to the article and approved the submitted version.

Conflict of interest statement

The authors declare that the research was conducted in the absence of any commercial or financial relationships that could be construed as a potential conflict of interest.

Appendix A. Supporting information

Supplementary data associated with this article can be found in the online version at doi:10.1016/j.biopha.2022.113171.

References

[1] A. Lightfoot, H.M. McGettrick, A.J. Iqbal, Vascular endothelial galectins in leukocyte trafficking, Front Immunol. 12 (2021), 687711.
[2] E.B. Okeke, J.E. Uzonna, The pivotal role of regulatory T cells in the regulation of innate immune cells, Front Immunol. 10 (2019) 680.
[3] G. Mamgain, et al., The role of microbiota in the development of cancer tumour cells and lymphoma of B and T cells, Cureus 13 (10) (2021), e19047.
[4] M.O. Brook, et al., Transplantation Without Overimmunosuppression (TWO) study protocol: a phase 2b randomised controlled single-centre trial of regulatory T cell therapy to facilitate immunosuppression reduction in living donor kidney transplant recipients, BMJ Open 12 (4) (2022), e061864.
[5] Z. Yousefi, et al., Dose-dependent effects of oleuropein administration on regulatory T-cells in patients with rheumatoid arthritis: an in vitro approach, Int J. Immunopathol. Pharm. 36 (2022), p. 3946320221086084.
[6] M. Mellado, et al., T Cell Migration in Rheumatoid Arthritis, Front Immunol. 6 (2015) 384.
[7] S. Nourshargh, R. Alon, Leukocyte migration into inflamed tissues, Immunity 41 (5) (2014) 694–707.
[8] Z. Fan, K. Ley, Leukocyte arrest: biomechanics and molecular mechanisms of beta2 integrin activation, Biorheology 52 (5–6) (2015) 353–377.
[9] F. Krautter, A.J. Iqbal, Glycans and glycan-binding proteins as regulators and potential targets in leukocyte recruitment, Front Cell Dev. Biol. 9 (2021), 624082.
[10] M. Schattner, Platelets and galectins, Ann. Transl. Med 2 (9) (2014) 85.
[11] D. Cooper, L.V. Norling, M. Perretti, Novel insights into the inhibitory effects of Galectin-1 on neutrophil recruitment under flow, J. Leukoc. Biol. 83 (6) (2008) 1459–1466.
[12] V. Eckardt, et al., Chemokines and galectins form heterodimers to modulate inflammation, EMBO Rep. 21 (4) (2020), e47852.

[13] B.R. Gittens, et al., Galectin-3: A Positive Regulator of Leukocyte Recruitment in the Inflamed Microcirculation, J. Immunol. 198 (11) (2017) 4458–4469.
[14] D. Cooper, et al., The effect of galectins on leukocyte trafficking in inflammation: sweet or sour? Ann. N. Y Acad. Sci. 1253 (2012) 181–192.
[15] X.W. He, et al., Serum levels of galectin-1, galectin-3, and galectin-9 are associated with large artery atherosclerotic stroke, Sci. Rep. 7 (2017) 40994.
[16] N. Bozorgmehr, et al., Galectin-9, a Player in cytokine release syndrome and a surrogate diagnostic biomarker in SARS-CoV-2 infection, mBio 12 (3) (2021).
[17] H. Yamamoto, et al., Induction of cell adhesion by galectin-8 and its target molecules in Jurkat T-cells, J. Biochem 143 (3) (2008) 311–324.
[18] M.J. O'Brien, et al., A unique role for galectin-9 in angiogenesis and inflammatory arthritis, Arthritis Res Ther. 20 (1) (2018) 31.
[19] A. Chakraborty, et al., Galectin-9 bridges human B cells to vascular endothelium while programming regulatory pathways, J. Autoimmun. 117 (2021), 102575.
[20] A.J. Iqbal, et al., Galectin-9 mediates neutrophil capture and adhesion in a CD44 and β2 integrin-dependent manner, Faseb J. 36 (1) (2022), e22065.
[21] P. Rochard, et al., Expression of the peripheral benzodiazepine receptor triggers thymocyte differentiation, Gene Expr. 12 (1) (2004) 13–27.
[22] C. Lhuillier, et al., Impact of exogenous galectin-9 on human T cells: contribution of the t cell receptor complex to antigen-independent activation but not to apoptosis induction, J. Biol. Chem. 290 (27) (2015) 16797–16811.
[23] A.A. Mansour, et al., Galectin-9 regulates monosodium urate crystal-induced gouty inflammation through the modulation of Treg/Th17 ratio, Front Immunol. 12 (2021), 762016.
[24] R. Yang, et al., Galectin-9 interacts with PD-1 and TIM-3 to regulate T cell death and is a target for cancer immunotherapy, Nat. Commun. 12 (1) (2021) 832.
[25] N. Nishi, et al., Development of highly stable galectins: truncation of the linker peptide confers protease-resistance on tandem-repeat type galectins, FEBS Lett. 579 (10) (2005) 2058–2064.
[26] C. Riedhammer, D. Halbritter, R. Weissert, Peripheral blood mononuclear cells: isolation, freezing, thawing, and culture, Methods Mol. Biol. 1304 (2016) 53–61.
[27] F. Maione, et al., Repetitive exposure of IL-17 into the murine air pouch favors the recruitment of inflammatory monocytes and the release of IL-16 and TREM-1 in the inflammatory fluids, Front Immunol. 9 (2018) 2752.
[28] T.S. Kapellos, et al., Cannabinoid receptor 2 deficiency exacerbates inflammation and neutrophil recruitment, Faseb J. 33 (5) (2019) 6154–6167.
[29] C. Cristiano, et al., Neutralization of IL-17 rescues amyloid-β-induced neuroinflammation and memory impairment, Br. J. Pharm. 176 (18) (2019) 3544–3557.
[30] A. Slater, et al., Structural characterization of a novel GPVI-nanobody complex reveals a biologically active domain-swapped GPVI dimer, Blood 137 (24) (2021) 3443–3453.
[31] Z. Zhi, et al., Galectin-9 activates platelet ITAM receptors glycoprotein VI and C-type lectin-like receptor-2, J. Thromb. Haemost. 20 (4) (2022) 936–950.
[32] M.I. Nielsen, et al., Galectin binding to cells and glycoproteins with genetically modified glycosylation reveals galectin-glycan specificities in a natural context, J. Biol. Chem. 293 (52) (2018) 20249–20262.
[33] E. Roux, et al., Fluid shear stress sensing by the endothelial layer, Front Physiol. 11 (2020) 861.
[34] S. John, R. Mishra, Galectin-9: from cell biology to complex disease dynamics, J. Biosci. 41 (3) (2016) 507–534.
[35] S. Oomizu, et al., Cell surface galectin-9 expressing Th cells regulate Th17 and Foxp3+ Treg development by galectin-9 secretion, PLoS One 7 (11) (2012), e48574.
[36] I. Okoye, et al., Galectin-9 expression defines exhausted T cells and impaired cytotoxic NK cells in patients with virus-associated solid tumors, J. Immunother. Cancer 8 (2) (2020).
[37] M.J. Gooden, et al., Galectin-9 activates and expands human T-helper 1 cells, PLoS One 8 (5) (2013), e65616.
[38] F. Nasri, et al., Oridonin could inhibit inflammation and T-cell immunoglobulin and mucin-3/Galectin-9 (TIM-3/Gal-9) autocrine loop in the acute myeloid leukemia cell line (U937) as compared to doxorubicin, Iran. J. Allergy Asthma Immunol. 19 (6) (2020) 602–611.
[39] S. Bi, et al., Galectin-9 binding to cell surface protein disulfide isomerase regulates the redox environment to enhance T-cell migration and HIV entry, Proc. Natl. Acad. Sci. USA 108 (26) (2011) 10650–10655.
[40] J.J. Grailer, M. Kodera, D.A. Steeber, L-selectin: role in regulating homeostasis and cutaneous inflammation, J. Dermatol. Sci. 56 (3) (2009) 141–147.
[41] M. Xingyuan, Z. Wenyun, W. Tianwen, Leukocyte function-associated antigen-1: structure, function and application prospects, Protein Pept. Lett. 13 (4) (2006) 397–400.
[42] R.L. Contento, et al., CXCR4-CCR5: a couple modulating T cell functions, Proc. Natl. Acad. Sci. USA 105 (29) (2008) 10101–10106.
[43] J. He, L.G. Baum, Endothelial cell expression of galectin-1 induced by prostate cancer cells inhibits T-cell transendothelial migration, Lab Invest 86 (6) (2006) 578–590.
[44] F. Krautter, et al., Characterisation of endogenous Galectin-1 and -9 expression in monocyte and macrophage subsets under resting and inflammatory conditions, Biomed. Pharm. 130 (2020), 110595.
[45] Y. Zhang, et al., Sialyl lewisx antigen-expressing human CD4+ T and CD8+ T cells as initial immune responders in memory phenotype subsets, J. Leukoc. Biol. 84 (3) (2008) 730–735.
[46] Y. Nishi, et al., Role of galectin-3 in human pulmonary fibrosis, Allergol. Int 56 (1) (2007) 57–65.
[47] A. Riva, et al., Soluble TIM3 and its ligands galectin-9 and CEACAM1 are in disequilibrium during alcohol-related liver disease and promote impairment of anti-bacterial immunity, Front Physiol. 12 (2021), 632502.
[48] N. Pang, et al., Activated Galectin-9/Tim3 promotes Treg and suppresses Th1 effector function in chronic lymphocytic leukemia, FASEB J. 35 (7) (2021), e21556.
[49] V.R. Wiersma, et al., Galectin-9 is a possible promoter of immunopathology in rheumatoid arthritis by activation of peptidyl arginine deiminase 4 (PAD-4) in granulocytes, Int J. Mol. Sci. 20 (16) (2019).
[50] K.M. Vilar, et al., Galectin-9 gene (LGALS9) polymorphisms are associated with rheumatoid arthritis in Brazilian patients, PLoS One 14 (10) (2019), e0223191.
[51] D. Weinmann, et al., Galectin-8 induces functional disease markers in human osteoarthritis and cooperates with galectins-1 and -3, Cell Mol. Life Sci. 75 (22) (2018) 4187–4205.
[52] P. von Hundelshausen, et al., The marriage of chemokines and galectins as functional heterodimers, Cell Mol. Life Sci. 78 (24) (2021) 8073–8095.
[53] H. Kaltner, et al., The sugar code: letters and vocabulary, writers, editors and readers and biosignificance of functional glycan-lectin pairing, Biochem J. 476 (18) (2019) 2623–2655.